PV Polaris – Automated PV System Orientation Prediction

Ernst Wittmann , Claudia Buerhop-Lutz , Savannah Bennett, Vincent Christlein , *Member, IEEE*, Jens Hauch , Christoph J. Brabec, and Ian Marius Peters

Abstract—The orientation of a photovoltaic system is an important parameter for power generation and yield predictions. Yet often, the real orientation is unknown. Measuring the orientation manually is time-consuming. This study introduces an automated Monte Carlo Search based algorithm called PV Polaris which is capable of predicting the systems orientation within 18 s, with uncertainties of less than 2° in tilt and 4° in azimuth. In terms of accuracy, PV Polaris outperforms other methods such as measurements with a tilt compensated compass or predictions from satellite images. Applicable at module, string and inverter levels, the algorithm only requires power monitoring data as well as an approximate coordinate as input. Additionally, the algorithm can operate inversely to estimate the system's coordinates based on a given orientation. By using this orientation prediction, it was possible to calculate the yearly yield loss due to non-ideal orientation. For photovoltaic systems we investigated, we found that yearly yield increases between 2.3% to 10.3% could be achieved if the PV systems orientation would be optimized.

Index Terms—Automated orientation prediction, PV orientation measurement, PV location prediction, monitoring data, PV polaris, performance optimization.

I. INTRODUCTION

IN RECENT years, solar photovoltaic (PV) energy has experienced substantial growth, with global installed capacity increasing from 480 gigawatts (GW) in 2018 to over 1000 GW in 2022. This growth is expected to continue, with projections indicating PV capacity could reach approximately 2800 GW by 2030 and 8500 GW by 2050. For most PV system owners, the primary objectives are either selling the produced electricity or reducing their own electricity costs [1]. To maximize the utility of solar modules, yield is important. Maximizing the energy yield of PV modules is a process influenced by module orientation.

Research highlights the impact of module orientation on energy output. Perez and Coleman [2] reported annual power gains of 10–40% through orientation optimization. Barbón et al. [3] found that tilt deviations of less than 10° from the optimal orientation result in minimal losses, while deviations of 21–23° and 43–47° lead to output losses of up to 5% and 20%, respectively.

Several studies have addressed optimal PV alignment. Mehleri et al. [4], used meteorological data and optimization models to identify orientations with maximum irradiation. Calabrò's algorithm [5] is based on global horizontal solar irradiation data measured by weather stations. Chen et al. [6] combined ground surface observations, satellite imagery, and weather station data to determine the angles with the highest irradiance.

To evaluate whether the orientation of a PV system can be improved, its current orientation must be determined. Manual measurements using tools such as levels or tilt-compensated compasses are time-consuming and pose safety risks. Alongside manual measurements, researchers have also developed non-contact orientation prediction methods. For instance, Meng et al. [7] and S. Killinger [8] used power signals combined with irradiance data or ambient temperature, achieving mean errors of 4–4.5° in azimuth and tilt. Saint-Drenan et al. [9] integrated power signals and meteorological data, achieving 2° accuracy in optimal conditions. Ruelle et al. [10] used a one diode array performance model to determine the orientation of PV systems, but without analysing the potential prediction error. K. Mason [11] trained a neural network to estimate the orientation by only using power recordings from inverter with a mean error of 2.6° in tilt and 4.7° in azimuth. Chen and Irwin [12] created SunDance, a black box approach requiring only two data points of the power generation from inverter during clear skies and the building location, achieving mean errors of ∼1.4° in tilt and ∼2.4° in azimuth.

Many existing methods rely on exogenous input data or are tailored for large-scale PV parks. In this study, we propose an optimisation-based method to determine fixed PV systems, orientations with the use of monitoring data. Our approach

Fig. 1.   Orientation of a PV system defined by two angles: tilt and azimuth.

Fig. 2.   On the left, simulations of PV systems with a 25° tilt and varying azimuth angles show shifts in start (S), peak (P), and end (E) times based on azimuth. On the right, simulations with a 120° azimuth and varying tilt angles reveal that increasing tilt shifts peak and end times earlier, while azimuths above 180° cause later start and peak times.
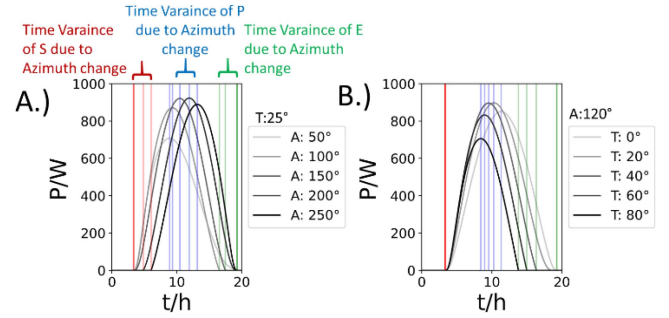
adapts simulation models to monitoring data (module, string or inverter), requiring only approximate coordinates of the PV system. The independence from external data sources like metrological data makes the algorithm applicable across a wide range of scenarios, from detailed module-level analysis to large-scale PV park evaluations. Additionally, the determined orientation is used to quantify potential performance improvements achievable through alignment optimization, providing actionable insights for enhancing PV system efficiency.

II. ORIENTATION OF A PV SYSTEM

The orientation of a PV system is defined by three angles: tilt, azimuth and rotation. The tilt represents the angle between the module's normal vector and the Earth's zenith. The azimuth is the angle between the module's norm vector and the geographic North Pole. The rotation is the angle around the module's norm vector (see Fig. 1). Since the rotation has no direct influence on the power generation of a PV system, it is excluded from this study. The tilt angle ranges from 0° (orthogonal to the zenith) to 90° (parallel to the zenith) and the azimuth from 0° to 360° (0°/360°: North, 90°: East, 180°: South, 270°: West).

The tilt and azimuth angles have an impact on the PV system's power output. For example, an east-facing PV module (azimuth ∼90°) starts, peaks, and ends power generation earlier than a west-facing one, because the module receives sunlight earlier, but loses the sunlight sooner (see Fig. 2(a)).

The timing of power generation—start, peak, and end times—can also be influenced by the tilt angle. For a horizontally oriented PV system (tilt = 0°), the azimuth angle is equivalent to the rotation of the system's normal vector and does not affect power generation, resulting in no time shift. If the azimuth angle is less than 180°, increasing the tilt angle shifts the peak and end times earlier (see Fig. 2(b)). For azimuth angles greater than 180°, a higher tilt angle delays the start and peak times. At an azimuth angle of 180°, increasing the tilt delays the start time and advances the end time. In addition to the time shifts the yield of the PV system changes with its orientation. The azimuth angle for highest yield production is always 180° (South), whereas the tilt angle for highest yield production changes with various factors like the system's latitude and climate.

III. ORIENTATION PREDICTION

To automatically predict the orientation of a PV system, a simulation is fitted to the system's monitoring data using the tilt and azimuth angle as fit parameters. To minimize prediction times and computational cost, the simulation assumes a defect free PV system operating under clear-sky conditions, described by the formula:

$$P_{sim}(t) = POA(t) \cdot \eta \cdot (1 + T_{coef} \cdot \Delta T(t)) \qquad (1)$$

with module efficiency η, temperature coefficient T_{coef}, the temperature difference $\Delta T(t)$ to standard test conditions (T = 25 °C), and the plane of array irradiance POA(t), calculated using established models. Five POA models were tested: Isotropic [13], [14], Simple Sandia [15], Hay and Davies [16], Reindl [17] and Perez [18] all based on the work of Ineichen and Perez [19] for the DNI, GHI and DHI as well as Reda and Andreas [20] for the sun position. Test results showed that a prediction based on the Isotropic model was the most accurate and the fastest.

Monitoring data can be recordings from modules, strings or inverter and, for purpose of this paper, must only include the power recordings over time. Unlike the simplified simulation, the power recordings include information as, for example, shading due to clouds, soiling or other factors, leading to variations in the power signal. The variation in the power signal leads to inaccurate predictions and thus the variations have to be filtered out. The most effective filtering method found uses three key times per day: the time of peak power and the first and last instances when a defined power threshold is exceeded. By compressing the monitoring data as well as the simulations on these three key times per day, it is not only possible to filter the data, but also to reduce the complexity of the simulation. Fig. 3 shows that only the location (latitude and longitude) as well as the orientation (tilt and azimuth angle) have influence on the three key times. All other simulation parameters ─ altitude, albedo, effectivity and temperature coefficient ─ can be ignored for the orientation predictions.

If orientation and monitoring data is available, the predictor can also be used to provide an estimate of the location. In case of the location prediction, only the start and end time are needed. In fact, the location prediction has proven to be more accurate
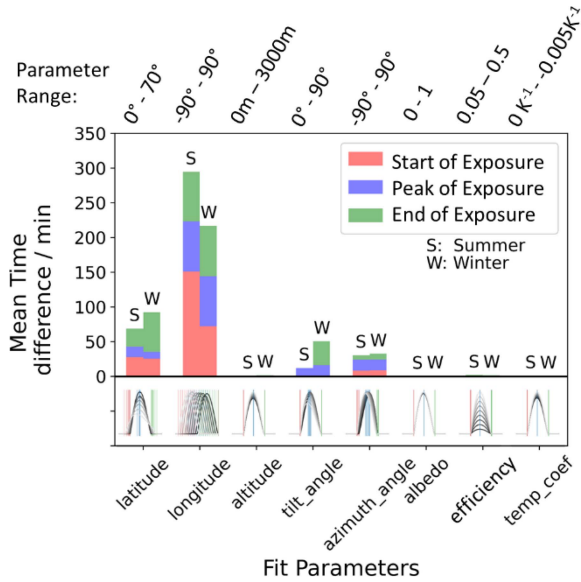
Fig. 3. Determination of the time variance of the key times (start-, peak- and end of exposure of the PV system) across the parameter ranges for summer and winter is visualized in a bar chart. Below the graph are the corresponding power generation simulations used to calculate the time variance. On top of the chart, the parameter ranges are listed. Results show that only the latitude, longitude, tilt and azimuth significantly affect the three key times.
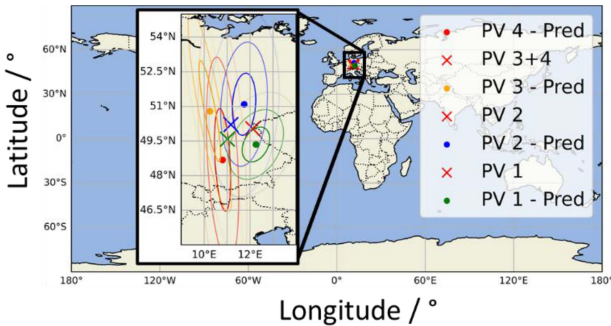

Fig. 4. If the orientation of a PV system is known, it is possible to use PV Polaris in reverse to predict an approximate location. The location prediction was tested on four PV systems, whereas two systems are next to each other, but with different orientations. The cross shows the real location and the dots the predictions. The ellipses around the dots represent the error range of 0.5σ, 1σ and 1.5σ.

if no peak times are given. An example were no peak time was included, is given in Fig. 4. With an avarage variance of 600 km in latitude and 60 km in longitude and an average distance of 125 km to the real location, the location prediction in the example performs well in comparison to the size of the world, but cannot be used to pinpoint the PV systems.

For acceptable key time calculations, the monitoring data should have a recording frequency of at least 15 min, or the data has to be interpolated to smaller frequencies in advance. Data from clear sky days are optimal for calculating the three key times. To identify clear-sky days, a clear sky day filter was developed for the monitoring data. The filter first removes all days with large gaps in the data or days not starting or ending with a power output of 0 W. The filter then generates a clear sky template following the approach of Peters et al. [21]. The

process involves finding the maximum power output for each time of day over a one-month dataset, multiplying the result by a percentile (e.g., 0.9 for Germany), and smoothing it using median and mean sliding windows. Each day in the dataset is compared to the template using correlation analysis, and days exceeding a user-defined correlation threshold are labeled as clear sky days. The clear sky days are interpolated to determine the peak as daily power maximum and the start and end time as first and last time when a manual definable percentage (power threshold) of the calculated maximum power is passed. The same method with the same power threshold is used for the simulation to determine the simulation start, peak and end time.

To fit the simulation to the monitoring data, three optimization algorithms: BOAR [22], Bayesian Optimization [23] and Monte Carlo Search (MCS) were tested. The results showed that all three methods achieved similar accuracy, but the Monte Carlo Search was significantly faster, operating more than twice as fast as Bayesian Optimization and over four times faster than BOAR. With a processing speed of 1.8 s per input day, MCS requires only 18 s to predict the orientation using data from 10 days (minimum of required days for accurate predictions). Due to its superior speed, MCS was selected as the optimization algorithm for orientation predictions.

For one iteration, the MCS chooses a random orientation and simulates each filtered clear sky day. Then the three key times of each simulated day are determined and compared with the three key times determined using the monitoring data, by calculating the time difference in minutes. For each day, the time differences are summed up and the mean value over all days is determined, giving the loss values. The MSC runs for 10 epochs, at 1000 iterations each. In the first epoch, it considers the full tilt and azimuth range (tilt: 0°–90° & azimuth 0°–360°). The following 9 epochs, the MCS in each epoch first halves the searching range, then takes the 10 orientations with lowest loss and, for each taken orientation, searches randomly 100 iterations around this point. The final orientation prediction is defined as the orientation with minimum loss over all iterations. In addition to the predicted orientation the prediction trend is also determined. For the prediction trend the best 1%, 3% and 5% of tested orientations are considered and the standard deviation in the form of an ellipse is calculated. An example of a prediction result can be seen in Fig. 5.

IV. MANUAL MEASUREMENT

To evaluate the orientation prediction, PV systems were measured manually using three different methods: Satellite Images (SI), Tilt Compensated Compass (TCC) and Level and Shadow Compass (LaSC). Each method has its advantages and disadvantages. Acquiring satellite images is beneficial as the PV system does not have to be accessed in person, but the prediction accuracy is unknown and tilt measurement is challenging.

The Tilt Compensated Compass available on most smartphones is placed on the PV modules and the tilt and azimuth angle can be recorded. Measuring the azimuth angle with the Tilt Compensated Compass can be inaccurate, since illuminated PV Modules create an electromagnetic field that interferes with
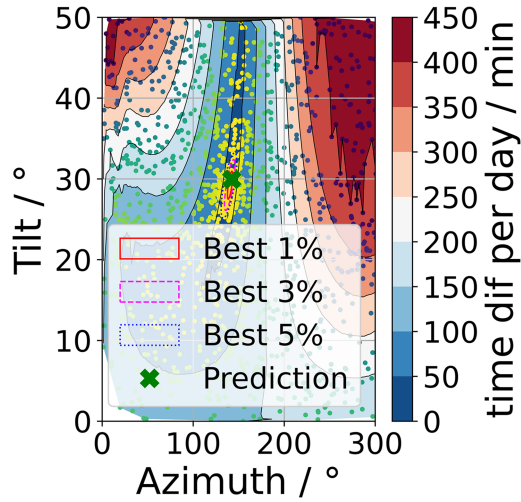
Fig. 5. Tilt over Azimuth prediction map via Monte Carlo Search. The scatter plot shows the tested orientations as data points and how close the key times of the prediction fit to the labels (yellow: very close, dark: far away). For the error ellipses, the best 1, 3 and 5% of orientation were taken into account.
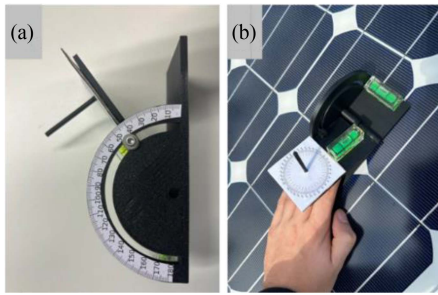

Fig. 6. 3D printed device to combine level and shadow compass. This device can be used to measure the tilt angle via two levels (a) and the azimuth angle via a shadow compass (b).

the device. On PV systems with metal support, even in the night the azimuth measurements with TCC are difficult, as the support is charged as a ferromagnet during the day.

The last method is the Level and Shadow Compass (see Fig. 6). The LaSC was already invented by the ancient Egyptians and still used by the Vikings for seamanship [24]. The LaSC method needs sun light and is therefore useable only during clear sky conditions. In comparison to the other methods, LaSC is the most time-consuming approach, but it is also the most accurate.

V. CLEAR SKY AND KEY TIME ANALYSIS

Initial tests revealed that the correlation value of the clear sky filter and the threshold for the start and end times impact the bias and accuracy of orientation predictions. The threshold for the start and end times depends on system-specific factors, such as shading. Shading can lead to incorrectly determined key times and, as a result, to faulty predictions. To bypass the shading influence, the threshold for the start and end time has to be adapted; e.g., if a the PV system is shaded by a big tree during the afternoon until sunset, the threshold has to be set to power outputs before the shading event occurs.
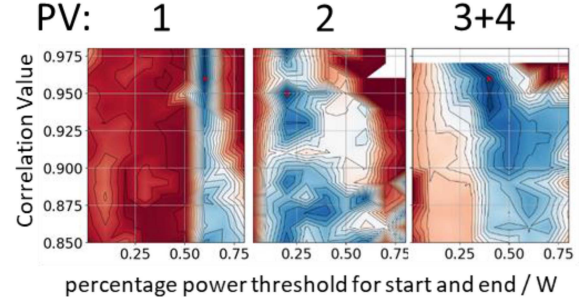

Fig. 7. Clear sky day finder parameter map. On all four PV parks the clear sky finder was used to filter clear sky days with different correlation values (0.85 - 0.99) and afterwards to determine the three key times via different start and end levels $(0.01 - 0.8\,V)$. Finally, the key times were used to predict the orientation and the mean square error to the real orientation was determined. Comparing all PV parks shows, that correlation parameters between 0.95 to 0.96 are generally good values. The key times depend on shading situations and are individual for each PV park, except 3 and 4 where the shading event occurs to almost the same times.

TABLE I
NUMBER OF MODULES, RECORDING TIME AND FREQUENCY OF EACH PV SYSTEM

PV system	Number of Modules	Recording Time	Recording Frequency
1	15	2019 - 2024	50 s
2	344	2020 - 2024	5 min
3	12	2021 - 2024	30 s
4	11	2021 - 2024	30 s

Fig. 7 shows that a correlation value of about 0.95 to 0.96 is adequate, as it provides a good balance between the quantity and quality of the input days. Higher correlation values may exclude too many days, resulting in a skewed distribution towards summer and leading to inaccurate tilt predictions. For an accurate forecast, there should be at least 10 clear sky days throughout the year. A low correlation value would include too many cloudy days, leading to critical key time calculation errors and inaccurate predictions.

VI. OBSERVED PV SYSTEMS

We investigated four PV systems of different sizes and orientations. The orientations were measured for every module in each PV system, using TCC, SI, and LaSC. All four PV systems were monitored on module and string/inverter level. The number of modules as well as the recording length and frequency can be seen in Table I. The recording frequency for all systems is higher than 15 min and, thus, is usable for the orientation prediction without preprocessing.

Comparing Table I with Fig. 8, it can be shown that with increasing recording time, there are more clear sky days accessible for each month. The error bars over the month show that even if the modules are standing edge to edge, the amount of recorded clear sky days over a month can vary up to five days.

PV system 1 has a total recording time of six years and the highest number of clear sky days totaling 167 days, followed by system 3 with 58 days, system 2 with 54 and system 4 with 25.
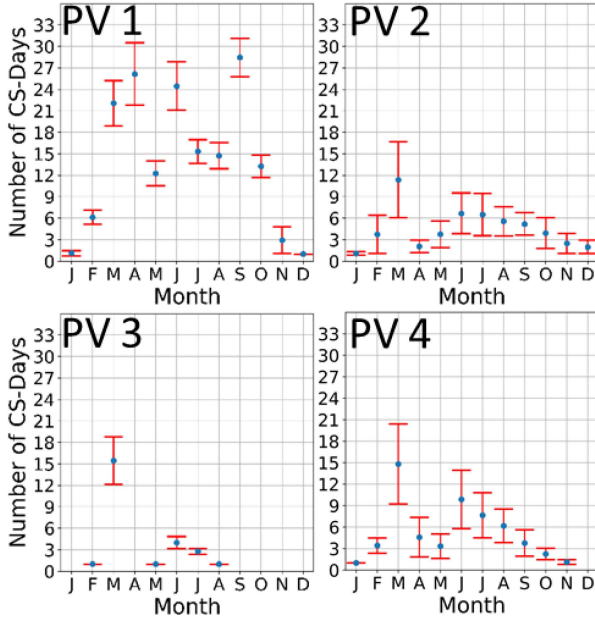
Fig. 8. Clear sky day distribution over the year. For each month the mean number of clear sky days as well as the standard deviation over all modules is given for each PV system.

The highest distribution of the clear sky days lies in spring and summer time, whereas there are very few or even no clear sky days in the winter.

VII. ORIENTATION PREDICTION RESULTS

The orientation predictions for the PV systems are shown in Fig. 9. A correlation value of 0.95 and the best threshold values for each system were used for the predictions. The prediction were performed with module (MP) and string (SP) monitoring data and are plotted together with the manual measurements via each measuring method. Below each plot a table is given with the resulting tilt and azimuth angle. As mentioned in Section V, it is assumed that the LaSC is the most accurate measurement and it is used as ground base.

For tilt prediction with a mean distance of 0.6° the closest method to LaSC is the TCC, followed by SP with 1.3° and MP with 1.7°. For the azimuth predictions, MP with a mean distance of 3° followed by SP with 4° outperforms SI with 10° and TCC with 19°. The worst predictions were performed for PV system 3. It is assumed, that system 3 performes worst, since it is the system with the lowest number of clear sky days and furthermore its existing clear sky days are all concentraded only to summer time. MP and SP have, for all PV systems the highest standard deviations except for PV system 4, where TCC measurement showed highest deviations due to strong electromagnetic fields interfering with the azimuth measurement. Compared to most related work, our approach achieves similar or better accuracy with less data input. The algorithm of Saint-Drenan et al. [9] achieves an accuracy of less than 2 degrees, but it requires meteorological data, whereas our approach does not need such data. The black box SunDance of Chen and Irwin [12] achieved better results with a mean error of ∼1.4° in tilt and ∼2.4° in

PV 1	Tilt	Azimuth
MP	28.3±4.8	224±5
SP	26.6±0.5	228±2
LaSC	27.7±0.4	226±1
TCC	27.6±0.3	256±1
SI		232±1

PV 2	Tilt	Azimuth
MP	14.5±5.5	191±15
SP	17.4±2.8	195±9
LaSC	16.7±1.3	199±3
TCC	17±3.3	192±7
SI		179±2

PV 3	Tilt	Azimuth
MP	33.7±4.7	147±23
SP	32.2±10	138±2
LaSC	31±0.4	145±0.6
TCC	32±0.7	142±1
SI		140±1

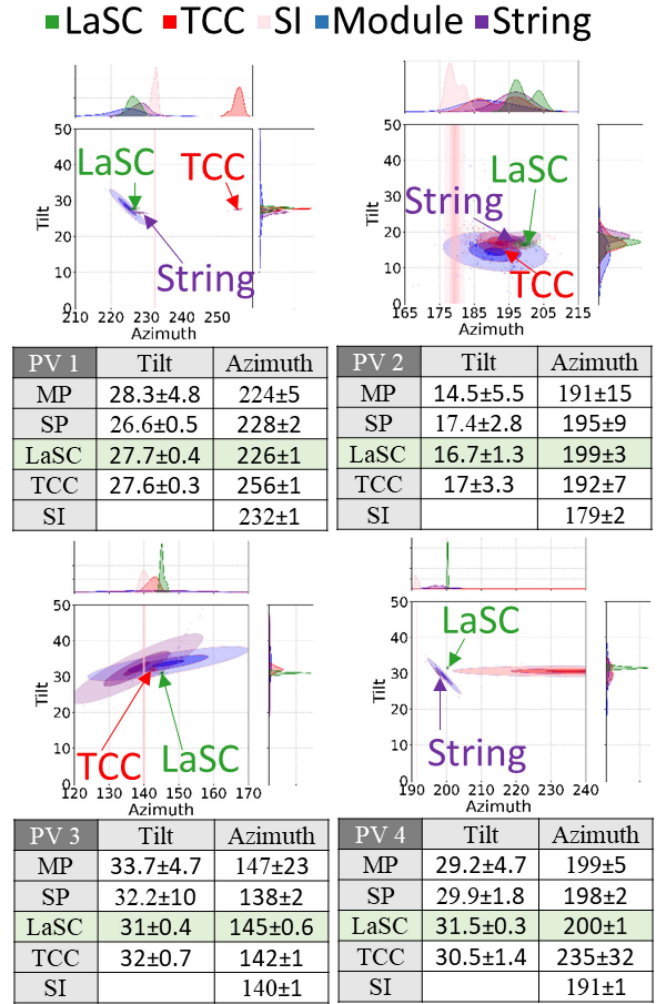| PV 4	Tilt	Azimuth
MP	29.2±4.7	199±5
SP	29.9±1.8	198±2
LaSC	31.5±0.3	200±1
TCC	30.5±1.4	235±32
SI		191±1

Fig. 9. Orientation prediction and measurements of all 4 PV systems. The prediction was performed via module and string/inverter data. Each method is plotted as an ellipse showing the 1σ, 2σ and 3σ range over the orientations of all modules. Among the plots the mean and standard deviations are listed for all methods.

azimuth, only requiring the systems location and two datapoints of behind-the-meter data. Since Sundance is based on behind-the-meter data, it can only determine the orientation of whole PV parks, whereas our approach can make use of module and string data and therefore gives a more comprehensive view into the PV parks.

VIII. USAGE OF ORIENTATION PREDICTION

With the predicted orientations, we fit the simulation described by formula 1 to the monitoring data from clear sky days, via the MCS. Alongside a simulated or manual set temperature, best fits are achieved if the monitoring data also includes the module temperature. Fitting the simulation reveals values for the temperature coefficient and efficiency. The predicted temperature coefficient had a mean distance of 0.0012 and the efficiency has a mean distance of 0.02 to the values of the manufacturer description. Next to the temperature coefficient and efficiency values we get a simulation that can be used to calculate the percental power loss over a day of the PV system. In Fig. 10,
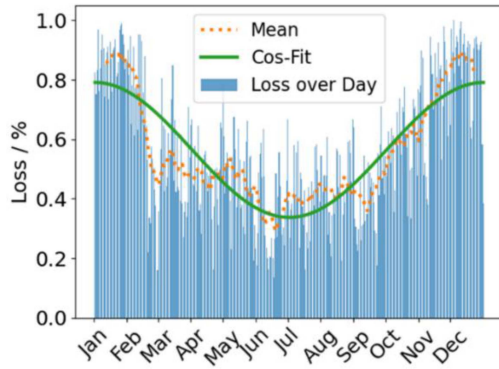
Fig. 10. Annual overview of daily power loss in percentage with included cos-fit. The fitted cos-function can be used to improve future predictions and to calculate the optimal orientation for a PV system.

TABLE II
PERCENTAGE POTENTIAL INCREASE IN POWER GENERATION THROUGH REORIENTATION FOR ALL PV PARKS

	PV 1	PV 2	PV 3	PV 4
Azimuth	226°	199°	145°	200°
Tilt	27.7°	16.7°	31°	31.5°
Estimated Best Tilt	34.6°	24.7°	36.5°	34.3°
LaSC in [%]	10.3 ± 0.4	5.3 ± 1.1	6.3 ± 0.2	2.3 ± 0.2
MP in [%]	9.6 ± 2.4	6.9 ± 4.6	8.3 ± 7.9	2.8 ± 1.9
SP in [%]	11.2 ± 0.8	4.7 ± 2.4	9.7 ± 1.2	2.4 ± 0.7

The actual azimuth and tilt angles are provided for reference. The optimal orientation, yielding the highest annual output, was determined through simulations incorporating daily power loss over the year. Measurements using the Level and Shadow Compass (LaSC) and predictions from module (MP) and string (SP) monitoring were compared to the optimal orientation to quantify the potential power gain.

the daily relative yield loss over a year of an observed PV system is shown. The loss rate is higher in winter than in summer. To simplify the result, a cosine function is fitted to the data.

By considering the loss rate, we can determine the optimal fixed orientation for maximum annual yield. The optimal azimuth angle for maximum yield is 180° (South). The optimal tilt angle depends on the location, yearly loss rate and self-shading loss. To add a rough estimation of the self-shading loss we used the work from D. Passias and B. Källbäck [25], which requires the height of the panel row and the distance between the rows.

To find the optimal tilt angle, we used a random walk algorithm, simulating different tilt angles over a year and factoring in the loss rates and self-shading loss. With the random walk, we calculated the optimal orientation for all 4 PV systems. In Table II, we can see, that the determined best tilt angles for single rowed PV systems lie between 34° and 37°, which is in a similar field to the literature values of 30° to 35° [26]. Explored systems could produce between 2.3% to 10.3% more yearly yield. Comparing the calculated yield increase via LaSC, MP and SP, we can see, that the maximal percentual difference lies at 3.4% and is due to a bad SP prediction led by a low number of available clear sky days concentrated to summer times. Taking the LaSC method as ground base, MP and SP performs with a mean error of 1.2%. In comparison to the mean orientation prediction error, the yield error is reduced, since the orientation

has less influence on the yield production than other parameters like the location.

IX. DISCUSSION

Based on the available data, PV Polaris was tested exclusively on fixed monofacial system types. In the following, we will discuss to what extent PV Polaris can also be applied to other system configurations.

Since the daily power profiles of monofacial and bifacial systems do not differ significantly, and the algorithm relies solely on three key times that are independent of the power output, we assume that the algorithm should also be applicable to fixed bifacial systems.

For systems with inverter clipping or tracking systems, however, a distinction must be made between orientation prediction and location prediction.

Location prediction does not necessarily require the peak time, as long as the start and end times of power production are available. In fact, testing the location prediction on PV systems with and without peak times resulted in slightly improved accuracy (approximately 1° in both latitude and longitude) when the peak times were omitted. We therefore assume that, provided the start and end times can be reliably determined, location prediction remains feasible for systems with inverter clipping as well as for tracking systems.

Orientation prediction, on the other hand, depends on the peak time and is therefore currently not applicable to systems affected by inverter clipping. To enable orientation prediction for such systems, the algorithm would need to be adapted. One possible approach could involve introducing a second, percentage-based power threshold to define two new key times immediately before and after the clipping event, replacing the peak time. Additionally, to effectively use the percentage-based threshold in systems with inverter clipping, a method for estimating the maximum possible daily power production in the absence of clipping would be required.

For tracking systems, orientation prediction as currently implemented is of limited applicability. Since the algorithm relies on three key times per day to infer a fixed orientation, it cannot determine the orientation of systems with continuously changing angles throughout the day. However, if one of the two orientation parameters — either tilt or azimuth — remains fixed, the algorithm may be capable of predicting this fixed parameter.

X. CONCLUSION

The orientation of a PV system can be described by the two angles, tilt and azimuth. Together with the location, the orientation is the only set of parameters that has significant influence on the key times of module power generation of a PV system during a day: start-, peak- and end- time. Given this fact, a simulation based on these key times can be used to predict the orientation of a PV module if the location is given or, vice versa, the location can be predicted if the orientation is known. To determine the key times, monitoring data given by module, string or inverter recordings, are filtered for clear sky days. The monitoring data should have at least a recording frequency of 15 min and 10 clear sky days distributed over the year for acceptable predictions.

The performance analysis of the tilt prediction resulted in a mean error of 2° and, thus, it is worse than a measurement by level (mean error 0.6°), but close to a measurement by mobile phone (mean error 1.7°). The main benefit, however, is that the prediction process is automated and does not require human intervention, saving time and money.

Measuring the azimuth angle is not a trivial task. Electromagnetic fields of the PV system can interfere with a normal or electrical compass (mean error 19°) and the accuracy of satellite images (mean error 10°) is unknown. The best method for measuring the azimuth angle manually is by making use of a shadow compass (mean error 1.4°). The prediction, with a mean error of 5°, is worse than a shadow compass, but outperformed the measurements via mobile phone or via satellite images.

In addition to the orientation prediction, the predictor can also be used to locate a PV system. The location prediction is within an average distance of 125 km – this cannot be used to pinpoint the exact location of the PV system, but it is adequate for an approximate location.

This paper has shown that, once the orientation of a PV system is determined, the yearly yield loss can be calculated. This yearly yield loss can then be used to determine the best orientation for each PV system. Each observed system could produce between 2 to 10% more yearly yield if the system is reorientated.

In summary, the proposed algorithm can be used to predict the PV system's orientation, to calculate the yearly yield loss due to suboptimal PV module orientation, and to determine the best orientation and the possible increased yearly yield should the system be reoriented.

XI. Outlook

There is room to improve the location and orientation prediction. Both predictions can be improved by better key time estimation. This paper makes only use of clear sky days to estimate the key times, but future work can be determining a method of including cloudy days in the prediction algorithm. By increasing the number of key times and improving the accuracy of key time estimation, the location and orientation prediction can be improved.

In addition to the orientation and location prediction the efficiency and temperature coefficient are also predictable.

XI. Declaration of Generative AI and AI-Assisted Technologies in the Writing Process

During the preparation of this work I (Ernst Wittmann) used
– Chat GPT to improve language and readability
– Deepl to improve language

After using these tools, I reviewed and edited the content as needed and take full responsibility for the content of the publication.

References

[1] "Tracking clean energy progess 2023," Assessing Critical Energy Technologies for Global Clean Energy Transitions, 2023. [Online]. Available: https://www.iea.org/reports/tracking-clean-energyprogress-2023

[2] R. Perez and S. Coleman, "PV module," *Home Power*, vol. 36, p. 16, 1993.

[3] A. Barbón, C. Bayón-Cueli, L. Bayón, and C. Rodríguez-Suanzes, "Analysis of the tilt and azimuth angles of photovoltaic systems in nonideal positions for urban applications," *Appl. Energy*, vol. 305, 2022, Art. no. 117802.

[4] E. D. Mehleri, P. L. Zervas, H. Sarimveis, J. A. Palyvos, and N. C. Markatos, "Determination of the optimal tilt angle and orientation for solar," *Renewable Energy*, vol. 35, pp. 2468–2475, 2010.

[5] E. Calabrò, "An Algorithm to Determine the Optimum Tilt Angle ofa Solar Panel from Global Horizontal Solar Radiation," *J. Renewable Energy*, vol. 2013, p. 12, 2013.

[6] X. Chen, Y. Lia, Z. Zhao, T. Ma, and R. Wanga, "General method to obtain recommended tilt and azimuth angles for photovoltaic systems worldwide," *Sol. Energy*, vol. 172, pp. 46–57, 2018.

[7] B. Meng, R. Loonen, and J. Hensen, "Data-driven inference of unkown tilt and azimuth of distributed PV systems," *Sol. Energy*, vol. 211, pp. 418–432, 2020.

[8] S. Killinger, N. Engerer, and M. B., "QCPB: A quality control algorithm for distributed photovoltaic array power output," *Sol. Energy*, vol. 143, pp. 120–131, 2017.

[9] Y. Saint-Drenan, Y. Bofinger, R. Fritz, S. Vogt, G. Good, and J. Dobschinski, "An empirical approach to parameterizing photovoltaic plants for power forecasting and simulation," *Sol. Energy*, vol. 120, pp. 479–493, 2015.

[10] V. Ruelle, M. Jeppesen, and M. Brear, "Rooftop PV model technical report," Melbourne Univ., 2016. [Online]. Available: https://aemo.com.au/-/media/files/electricity/nem/planning_and_forecasting/demand-forecasts/nefr/2016/uomrooftop-pv-model-technical-report.pdf

[11] K. Mason, M. J. Reno, L. Blakely, S. Vejdan, and S. Grijalava, "A deep neural network approach for behind-the-meter residential PV size, tilt and azimuth estimation," *Sol. Energy*, vol. 196, pp. 260–269, 2020.

[12] D. Chen and D. Irwin, "SunDance: Black-box behind-the-meter solar disaggregation," *Sol. Disaggregation*, vol. 17, pp. 16–19, 2017.

[13] H. Hottel and B. Woertz, "Evaluation of flat-plate solar heat collector," ASME, vol. 64, p. 91, 1942.

[14] P. Loutzenhiser et al., "Empirical validation of models to compute solar irradiance on inclined surfaces for building energy simulation," *Sol. Energy*, vol. 81, pp. 254–267, 2007.

[15] M. Lave, W. Hayes, A. Pohl, and C. W. Hansen, "Evaluation of global horizontal irradiance to plane-of-array irradiance models at locations across the United States," *IEEE J. Photovolt.*, vol. 5, no. 2, pp. 597–606, Mar. 2015.

[16] J. Hay and D. J.A., "Calculations of the solar radiation incident on an inclined surface," in *Proc. 1st Can. Sol. Radiat. Data Workshop*, 1980, p. 59.

[17] D. Reindl, W. A. Beckmann, and J. A. Duffie, "Diffuse fraction correlations," *Solar Energy*, vol. 45, no. 1, pp. 1–7, 1990.

[18] R. Perez, R. Seals, P. Ineichen, R. Stewart, D. Menicucci, "A new simplified version ot the Perez diffuse irradiance model for tilted surfaces," *Solar Energy*, vol. 39, no. 3, pp. 221–232, 2007.

[19] P. Ineichen and R. Perez, "A new airmass independent formulation for the linke," *Sol. Energy*, vol. 73, pp. 151–157, 2002.

[20] I. Reda, A. Andreas, "Solar position algorithm for solar radiation applications," *Solar Energy*, vol. 76, no. 5, pp. 577–589, 2005.

[21] I. M. Peters, S. Karthik, L. Haohui, T. Buonassisi, and A. Nobre, "Urban haze and photovoltaics," *Energy Environ. Sci.*, vol. 11, pp. 3043–3054, 2018.

[22] L. L. Vincent and M. Le Corre, "BOAR: Bayesian optimization for automated research," GitHub. [Online]. Available: https://github.com/i-MEET/boar

[23] F. Nogueira, "Bayesian optimization: Open source constrained global optimization tool for Python," *Int. J. Comput.-Aided Eng. Softw.*, 2014. [Online]. Available: https://github.com/bayesian-optimization/BayesianOptimization

[24] B. Bernáth, "How could the Viking Sun compass be used with sunstones before and after sunset? Twilight board as a new interpretation of the Uunartoq artefact fragment," *Proc. Math., Phys., Eng. Sci.*, vol. 470, no. 2166, 2014, Art. no. 20130787.

[25] D. Passias and B. Källbäck, "Shading effects in rows of solar cell panels," *Sol. Cells*, vol. 11, pp. 281–291, 1984.

[26] Y.-M. Saint-Drenan, L. Wald, T. Ranchin, L. Dubus, and A. Troccoli, "An approach for the estimation of the aggregated photovoltaic power generated in several European countries from meteorological data," *Adv. Sci. Res.*, vol. 15, pp. 51–62, 2018.